

Comparison of conventional and garnet-aluminosilicate-quartz O isotope thermometry: Insights for mineral equilibration in metamorphic rocks

DAVID P. MOECHER^{1,*} AND ZACHARY D. SHARP^{2,†}

¹Department of Geological Sciences, University of Kentucky, Lexington, Kentucky 40506, U.S.A.

²Institut de Minéralogie et Pétrographie, Université de Lausanne, CH-1015 Lausanne, Switzerland

ABSTRACT

Oxygen isotope thermometry based on fractionations among quartz, garnet, kyanite, sillimanite, and potassium feldspar in amphibolite to granulite facies schists and gneisses was compared to thermometry based on mineral equilibria (“conventional thermometry”). The former approach takes advantage of the exchange between quartz and more refractory minerals such as garnet and the aluminosilicates, and their potential for preserving peak oxygen isotopic fractionations. Although isotopic thermometry using these phases is potentially an approach for circumventing the problem in slowly cooled rocks of retrograde oxygen isotopic exchange with micas and feldspars, and of Fe and Mg exchange between garnet and biotite, the results are accurate or geologically meaningful in only certain settings. In most cases, the results of isotopic thermometry must be evaluated with the aid of quantitative forward models for calculating the amount of retrograde diffusive exchange among micas, feldspars, and quartz. Two models used here predict quartz isotopic compositions that differ by only 0.1 per mil and, in most cases, reproduce to within 0.2 per mil the measured isotopic composition of quartz. Excellent agreement between isotopic and conventional thermometry is obtained for mid-to-upper amphibolite facies rocks that have experienced one period of recrystallization and mineral growth, and if they are coarse-grained or cooled in the absence of a hydrous fluid phase. Isotopic temperatures of 850 °C are in excellent agreement with conventional thermometry in migmatitic granulite facies metapelites if cooling occurred under anhydrous conditions. In other cases, isotopic temperatures in granulite facies rocks are higher than conventional temperatures, a reasonable result in view of the tendency for retrograde cation exchange between garnet and biotite. In samples that have undergone multiple periods of recrystallization or metamorphism, isotopic temperatures from coexisting quartz, garnet, and aluminosilicates may be modified by diffusional exchange of quartz with micas and feldspars aided by recrystallization, by retrograde reactions involving the latter phases, or by open-system interaction with externally derived fluids. External fluid infiltration, combined with recrystallization of quartz and aluminosilicate, may result in isotopic reversals between garnet and matrix phases. Conventional thermobarometry in such complex rocks, based in large part on mineral equilibria involving garnet, may be erroneously assigned geological significance in the absence of insights provided by oxygen isotope analysis.

INTRODUCTION

The evolution of mountain belts is commonly viewed by petrologists in terms of changes in pressure and temperature experienced by rocks as they are loaded, heated, exhumed, and cooled during an orogenic cycle (i.e., the pressure-temperature-time path; e.g., England and Thompson 1984). Estimating the pressure and temperature attending peak metamorphism, and changes in these parameters with time, is a fundamental goal of petrology and principal constraint on models of evolution of the crust. Considerable progress has been made in the last decade in accurate calibration of mineral equilibria and in methods for accurate measurement of major element mineral

compositions and thermodynamic properties, presumably enhancing the accuracy of geothermobarometric calculations (Holland and Powell 1990; Berman 1991). Although the precision of many pressure and temperature determinations is probably very good ($< \pm 50$ °C), few methods exist for assessing the accuracy of these determinations because sources of error are covariant and not normally distributed (Hodges and McKenna 1987; Berman 1991; Kohn and Spear 1991). Phase equilibrium constraints and petrogenetic grids provide one way to assess accuracy, but these approaches are not independent constraints as they are based on the same experimental and thermodynamic databases as thermobarometric calibrations.

Thermobarometric calculations in pelitic metamorphic rocks are based primarily on partitioning of cations or phase components among garnet, aluminosilicates, micas, and feldspars (herein referred to as “conventional thermobarometry”), with the concentration of components measured by electron probe

*E-mail: moker@pop.uky.edu

†Present address: Department of Earth and Planetary Sciences, University of New Mexico, Albuquerque, New Mexico 87131-1116, U.S.A.; E-mail: zsharp@unm.edu

microanalysis. Oxygen isotope fractionations among metamorphic minerals—oxygen isotope thermometry—is a powerful alternative to conventional thermometry (Clayton and Epstein 1961; O'Neil and Clayton 1964; Farquhar et al. 1993), and provides an *independent* means of assessing the accuracy of conventional methods. Both approaches have drawbacks. The most serious is resetting or exchange of components or isotopes among minerals during slow cooling following peak metamorphism (Bowman and Ghent 1986; Giletti 1986; Sharp 1988; Spear and Florence 1992) or as a result of retrograde net-transfer mineral reactions (Chamberlain et al. 1990; Kohn 1993; Young 1993). However, judicious selection of samples can circumvent such problems (Spear 1991; Eiler et al. 1993; Farquhar et al. 1993).

The development of the laser heating technique for extraction of oxygen from refractory minerals with very slow diffusion rates for oxygen (garnet, kyanite, sillimanite, staurolite, zircon) provides a means for retrieving peak oxygen isotope fractionations and temperatures from metamorphic index minerals (Sharp 1995; Valley et al. 1994). In addition, oxygen isotope analysis provides a means for assessing which phases are in isotopic equilibrium and thus may have equilibrated with regard to major chemical components as well. The fundamental assumption of chemical equilibrium in conventional thermobarometry may be valid in rocks that have experienced a single period of metamorphic crystallization. It may not be valid for rocks that have undergone polymetamorphism or periods of deformation and recrystallization without new mineral growth.

This study is a comparison of conventional and stable oxygen isotope thermometric methods applied to regional mono- and polymetamorphic pelitic rocks from various localities in the Appalachian Orogen of southern New England and western North Carolina. In addition to providing an independent assessment of conventional geothermometry, oxygen isotope analysis provides surprising insights into attainment of isotopic and chemical equilibrium among minerals in rocks that have undergone deformation and recrystallization following growth of aluminosilicate and garnet porphyroblasts.

METHODS

Quartz, garnet, either kyanite or sillimanite, and in one case potassium feldspar were separated from medium- to high-grade metapelitic schists and gneisses, and reacted by the laser fluorination technique to extract oxygen for stable isotope analysis at the University of Lausanne following the methods of Sharp (1995). One to two milligrams of sample were analyzed in duplicate. All minerals from the same sample were analyzed during the same session to minimize possible inter-run experimental drift. Typical precision (1σ), based on analytical reproducibility, varied from ± 0.01 to 0.1 per mil for garnet and aluminosilicates, and from ± 0.05 to 0.3 per mil for quartz (Table 1). Repeated analysis of an internal laboratory quartz standard calibrated against NBS-28 quartz yielded 18.2 ± 0.2 (1σ) per mil [accepted value is 18.2 per mil vs. standard mean ocean water (SMOW)]. No systematic correction of measured values was necessary. All isotope values are presented in terms of $\delta^{18}\text{O}$ notation in per mil differences relative to SMOW, where the $\delta^{18}\text{O}$ values of NBS-18 and NBS-19 are 9.65 and 2.2 per mil, respectively ($\alpha_{25\text{C}} = 1.01025$).

Electron probe microanalysis of all phases was carried out on an ARL SEMQ instrument at 15 kV and 10 (feldspar, mica) or 20 nA (garnet) at the University of Kentucky. Raw X-ray counts were reduced using the ZAF option of the PRSUPR microprobe analytical package of Donovan et al. (1991). The latter software permits use of various combinations of silicate standards during a single run to assess the accuracy of microprobe analysis as determined by oxide sums, mineral formulae, and reproduction of secondary standards. Compositional zoning was assessed in all garnets by performing microprobe traverses in two directions across garnet porphyroblasts. Analytical precision and the degree of homogeneity among matrix phases was assessed by analyzing up to 10 grains of each phase in various textural relationships with other phases. The results of the microanalyses are presented in Appendix A and in a companion publication (Moecher 1999).

Isotopic temperature estimates were determined from the temperature-dependent isotope fractionation factors among quartz (Qtz) (all mineral abbreviations after Kretz 1983), garnet (Grt) and aluminosilicates (Als) derived by Sharp (1995) using a value for $A_{\text{Qtz-Grt}}$ derived from various empirical, theoretical, and experimental studies. Temperatures were calculated from the relation

$$(1000\ln\alpha_{\text{A-B}} = A 10^6/T^2) \quad (1)$$

from the average isotopic composition of respective phases in each exchange pair (Qtz-Als, Qtz-Grt, Als-Grt). Propagation of an analytical precision of ± 0.2 per mil through Equation 1 ($1000\ln\alpha_{\text{A-B}}$ approximated as $\Delta_{\text{A-B}} = \delta^{18}\text{O}_{\text{A}} - \delta^{18}\text{O}_{\text{B}}$) yields a temperature uncertainty of ± 30 °C for the Qtz-Grt exchange, ± 40 °C for the Qtz-Als exchange, and ± 100 °C for the aluminosilicate-garnet exchange.

In a closed system, temperature estimates derived from oxygen isotope fractionations involving quartz, even fractionations with slowly diffusing minerals such as aluminosilicates and garnet, yield minimum estimates of peak temperature. This is due to retrograde isotopic exchange of quartz with minerals possessing lower closure temperatures for oxygen diffusion that are common in metapelites (plagioclase, muscovite, biotite, and potassium feldspar; Giletti 1986). Retrograde exchange with other minerals in any closed system will cause the $\delta^{18}\text{O}$ value of quartz to increase because quartz fractionates ^{18}O relative to other minerals. Thus, measured values of $\Delta^{18}\text{O}_{\text{Qtz-Grt}}$ and $\Delta^{18}\text{O}_{\text{Qtz-Als}}$ are *maxima* and yield temperature estimates that are *minima*. It is important to assess the extent and conditions (hydrous vs. anhydrous) of the retrograde exchange using available quantitative models that explicitly account for factors controlling retrograde diffusional exchange (Giletti 1986; Eiler et al. 1992, 1994; Jenkin et al. 1994). This has been done using the program "COOL" (Jenkin et al. 1991), which is essentially an encoded version of the analytical approach of Giletti (1986) for modeling retrograde diffusive isotopic exchange. We have also modeled the retrograde cooling and exchange history using the "Fast Grain Boundary" model and computer program ("FGB") of Eiler et al. (1992, 1994).

Due to extremely slow diffusion rates for oxygen in kyanite and garnet, and their tendency not to recrystallize during periods of deformation following growth, these phases ideally could

TABLE 1. Oxygen isotope compositions, fractionations, and temperatures*

Sample no. Lithol. (Als polymorph)	$\delta^{18}\text{O}_{\text{SMOW}}$			$\Delta^{18}\text{O}$			T (°C)			T °C/P kbar
	Quartz	Als	Garnet	Qtz-Grt	Qtz-Als	Als-Grt	Qtz-Grt	Qtz-Als	Als-Grt	Conventional
Pelham										
1: schist (Ky)	15.38	12.89	11.85							
	15.75	12.90	11.95							
	15.46									
Avg	15.53	12.89	11.90	3.63	2.64	0.99	650	650	655	650/7
2: gneiss (Sil)	14.88	12.93	12.21							
	15.14	12.88	12.24							
Avg	15.01	12.90	12.21	2.81	2.11	0.70	780	760	830	750/5
Waterbury										
3: schist (Ky)	15.21	12.00	10.94							
	15.05	—	10.91							
Avg	15.13	12.00	10.93	4.21	3.14	1.07	585	575	620	550/4
4: schist (Ky)	14.97	12.53	11.81							
	14.94	12.45	11.81							
Avg	14.95	12.49	11.81	3.14	2.46	0.68	720	680	850	700/8
5: gneiss (Ky)	13.38	10.29	9.10							
	13.69	10.01	9.24							
Avg	13.54	10.15	9.17	4.37	3.38	0.99	570	540	655	560/4
6: schist (Ky)	13.29	9.64	8.88							
	13.25	—	8.86							
Avg	13.27	9.64	8.87	4.40	3.63	0.77	570	510	775	na
Willimantic										
7: gneiss (Sil)	13.98	11.96	11.06							
	13.79	11.94	11.12							
Avg	13.89	11.95	11.09	2.89	2.03	0.86	760	780	720	710/5.5
8: schist (Ky)	12.82	9.34	10.93							
	12.77	9.31	10.92							
Avg	12.79	9.32	10.92	1.87	3.47	-1.60	1015	530	na	600/4
9: schist (Ky)	13.48	10.20	10.15							
	13.41	10.24	10.11							
Avg	13.44	10.22	10.13	3.31	3.22	0.09	695	565	2845	560/3.5
W. Blue Ridge										
	Kfs	Als	Grt	Kfs-Grt	Kfs-Als	Als-Grt	Kfs-Grt	Kfs-Als	Als-Grt	
10: schist (Sil)	9.55	8.54	7.82	1.73	1.01	0.72	837	853	814	850/9
Saskatchewan										
	Qtz	Ky	Grt	Qtz-Grt	Qtz-Als	Als-Grt	Qtz-Grt	Qtz-Als	Als-Grt	
11: gneiss (Ky)	10.05	7.52	11.45	-1.40	2.39	-3.80	na	700	na	na
	10.00	7.78								
	10.06									
Avg	10.04	7.65	na							

* Temperature-dependent fractionation factors: $1000\ln\alpha(\text{Qtz-Als}) = 2.25 \cdot 10^6/T^2$; $1000\ln\alpha(\text{Qtz-Grt}) = 3.1 \cdot 10^6/T^2$; $1000\ln\alpha(\text{Als-Grt}) = 0.85 \cdot 10^6/T^2$; $1000\ln\alpha(\text{Kfs-Als}) = 1.28 \cdot 10^6/T^2$; $1000\ln\alpha(\text{Kfs-Grt}) = 2.13 \cdot 10^6/T^2$ (Sharp 1995; Bottinga and Javoy 1973).

be used to “see through” the effects on quartz isotopic compositions of retrograde cooling and fabric recrystallization. Although the relatively small Als-Grt fractionation makes this approach relatively imprecise, it will be seen that in some cases the Ky-Grt fractionation yields temperatures that are consistent (± 50 °C) with fractionations involving quartz.

Because not all minerals in each sample were analyzed for their oxygen isotope composition, the extent of retrograde isotopic exchange among minerals was monitored using the isotopic composition of quartz. That is, quartz will reset by diffusional exchange with micas and feldspars to varying degrees depending on cooling rate, grain size, initial temperature, and whether cooling occurred in the presence or absence of a hydrous fluid phase. A more accurate assessment of the retrograde exchange history of a rock would be obtained by measuring the isotopic composition of all phases and comparing the measured values with those obtained by modeling the process of retrograde diffusion and exchange (e.g., Farquhar et al. 1996).

Diffusion parameters used in modeling are listed in Tables 2 and 3, and modes, grain sizes, and cooling rates are compiled in

Table 3. In the following calculations, aluminosilicate or garnet were used to calculate the peak isotopic composition of quartz at the inferred peak temperature, using the Qtz-Als and/or Qtz-Grt fractionation factors of Sharp (1995). Aluminosilicates and garnet were excluded from the calculation of isotopic exchange due to slow oxygen diffusion that renders these minerals closed to diffusional exchange upon cooling even at granulite facies temperatures (Fortier and Giletti 1989; Young 1993). Model quartz isotopic compositions derived from COOL and FGB agree to within 0.1 per mil (Table 3).

Numerous studies have evaluated quantitatively the relative effects of mode, grain size, cooling rate, and diffusion parameters (pre-exponential factor D_0 ; activation energy Q) on the isotopic composition of minerals during cooling (Giletti 1986; Eiler et al. 1993; Jenkin et al. 1994; Massey et al. 1994; Farquhar et al. 1996; Ghent and Valley 1998). It was found here that uncertainties in modes of 10% (absolute) and in grain size and cooling rate of a factor of 2 correspond to uncertainties in mineral oxygen isotopic compositions of only 0.1 to 0.2 per mil. In contrast, the modeled isotopic composition of quartz and feld-

TABLE 2. Data used in modeling retrograde exchange history

	D_0 (cm ² /s)	Q (kJ/mol)	Shape factor	Ref.	$1000\ln\alpha_{(Qtz-Min)}$	Ref.
α -Quartz			8.7			
hydrous		190	284	1		
anhydrous	2.1×10^{-8}	159		2		
β -Quartz			8.7			
hydrous	4×10^{-7}	142		1		
anhydrous	2.1×10^{-8}	159		2		
Plagioclase			55		$1.3 \times 10^6/T^2$	7
hydrous	1.4×10^{-7}	110		3		
anhydrous	1×10^{-5}	236		4		
Muscovite	7.7×10^{-5}	163	27	5	$1.0 \times 10^6/T^2 + 0.6$	7
Biotite	9.1×10^{-6}	142	27	5	$2.2 \times 10^6/T^2$	8
Potassium feldspar			55		$1.0 \times 10^6/T^2$	9
hydrous	4.5×10^{-8}	107		3		
anhydrous	1×10^{-5}	236		6		

Note: (1) Giletti and Yund 1984; (2) Sharp et al. 1991; (3) Giletti et al. 1978; (4) Elphick et al. 1988; (5) Fortier and Giletti 1991; (6) assumed equal to anhydrous diffusion in anorthite; (7) Bottinga and Javoy 1973; (8) Chacko et al. 1996; (9) Bottinga and Javoy 1973.

TABLE 3. Modal and grain size input data for modeled samples, and results of modeling

Sample	Mineral	Mode	Grain dia. (mm)	Cooling rate (%/m.y.)	Initial T (°C)	$\delta^{18}O$ Qtz calc. (wet)	$\delta^{18}O$ Qtz calc. (dry)		$\delta^{18}O$ Qtz measured (1 σ)
							COOL	FGB	
Pelham									
1: schist	Qtz	0.39	2	20	650	16.4	15.6	15.6	15.5 (0.2)
	PI	0.11	2						
	Ms	0.28	1						
	Bt	0.22	1						
2: gneiss	Qtz	0.40	1	10	825	15.6	15.2	15.3	15.0 (0.1)
	PI	0.30	0.5						
	Bt	0.30	0.5						
Waterbury									
3: schist	Qtz	0.47	1	7.5	700	14.8	14.5	14.5	15.1 (0.1)
	PI	0.05	1						
	Ms	0.26	1						
	Bt	0.21	1						
4: schist	Qtz	0.31	5	7.5	700	15.7	15.0	15.0	15.0 (0.02)
	PI	0.06	5						
	Ms	0.27	3						
	Bt	0.27	3						
5: gneiss	Qtz	0.31	0.2	7.5	550	13.9	13.7	13.8	13.5 (0.2)
	PI	0.06	0.2						
	Ms	0.06	0.5						
	Bt	0.32	0.5						
6: schist	Qtz	0.33	0.5	7.5	550	13.8	13.5	13.4	13.3 (0.02)
	Ms	0.27	0.5						
	Bt	0.40	0.5						
	Kfs	0.25	0.2						
Willimantic									
7: gneiss	Qtz	0.61	1	10	825	14.6	14.1	14.1	13.9 (0.1)
	PI	0.22	0.5						
	Kfs	0.11	1						
	Bt	0.06	0.25						
8: schist	Qtz	0.38	1	10	550	13.0	12.6	12.7	12.8 (0.03)
	PI	0.06	0.5						
	Ms	0.12	0.5						
	Bt	0.44	1						
9: schist	Qtz	0.44	0.5	10	550	14.5	13.6	13.6	13.4 (0.04)
	PI	0.17	0.5						
	Ms	0.11	0.25						
	Bt	0.28	0.25						
Blue Ridge									
WSG93.1 schist	Kfs	0.75	2	10	900	10.2	9.6	9.7	9.6 (na)
	Bt	0.25	1						

spars may change drastically (~1–2 per mil) or very little if at all (~0.1 per mil), depending on whether one uses diffusion data for quartz and feldspars measured under hydrous ($P_{H_2O} = P_{total}$) or anhydrous ($P_{H_2O} = 0$, $P_{total} = P_{CO_2}$ or P_{O_2}) experimental conditions, respectively (e.g., Elphick et al. 1988). Calculations

were carried out with both sets of data permitting assessment of the presence or absence of a hydrous fluid phase during post-peak metamorphic cooling and retrograde isotopic exchange (e.g., Sharp and Moecher 1994).

Diffusion data for micas have only been measured under

experimental conditions of $P_{\text{H}_2\text{O}} = P_{\text{total}}$. We have used these values for model calculations simulating anhydrous cooling as well. Ghent and Valley (1998) suggested that such an application is unwarranted. However, use of the mica data provides upper limits on the degree of resetting because oxygen diffusion in silicates is slower under anhydrous conditions compared to hydrous conditions, assuming the diffusion mechanism in micas is the same as in quartz and feldspar.

Oxygen isotope fractionation factors among minerals common to metapelitic rocks have been determined empirically (e.g., Bottinga and Javoy 1973; Sharp 1995), calculated from theoretical principles (e.g., Kieffer 1982; Hoffbauer et al. 1994), and measured experimentally (e.g., Clayton et al. 1989; Chacko et al. 1996). The choice of fractionation factors affects temperature estimates and model calculations if a mineral is modally abundant. The Qtz-Bt fractionation factor of Bottinga and Javoy (1973) is much larger than that derived from the data of Chacko et al. (1996) on Bt-Cc exchange combined with the experimental Qtz-Cc fractionation factors of Clayton et al. (1989) (4.25 vs. 2.83 per mil, respectively, at 600 °C). However, the Qtz-Ms and Qtz-Pl fractionation factors of Bottinga and Javoy (1973) yield fractionations in the temperature interval of interest here (800 to 500 °C) that are analytically unresolvable (Qtz-Ms = 1.91 vs. 1.80 per mil; Qtz-Pl(An₃₅) = 1.75 vs. 1.72 per mil at 600 °C) from the experimental data of Chacko et al. (1996) and Clayton et al. (1989). Although there is a large difference in Qtz-Bt fractionations, it was found that empirical fractionation factors yield modeled quartz isotopic compositions that are only 0.1–0.2 per mil different than when using the experimental values. This small difference is due to the fact that biotite never dominates the mode in any of the samples studied.

Conventional geothermometry and geobarometry calculations are based on the thermodynamic data base and garnet activity-composition relations of Berman (1988, 1990). The TWEEQU approach (Berman 1991) was used when an appropriate number of phases were present to calculate the *P-T* locus of all possible equilibria among selected phase components (typically almandine, pyrope, grossular, annite, phlogopite, muscovite, kyanite/sillimanite, anorthite, quartz). The reactions used include:

1. Almandine + Phlogopite = Annite + Pyrope
2. Almandine + Muscovite + Grossular = Annite + 3 Anorthite
3. Pyrope + Muscovite + Grossular = Phlogopite + 3 Anorthite
4. 3 Anorthite = Grossular + 2 Al₂SiO₅ + 3 Quartz
5. Almandine + Muscovite = Annite + 2 Al₂SiO₅ + Quartz
6. Pyrope + Muscovite = Phlogopite + 2 Al₂SiO₅ + Quartz
7. Almandine + 3 Rutile = 3 Ilmenite + Al₂SiO₅ + 2 Quartz
8. Grossular + 2 Almandine + 6 Rutile = 3 Anorthite + 6 Ilmenite + 3 Quartz
9. 2 Grossular + Almandine + 3 Rutile + 3 Al₂SiO₅ = 6 Anorthite + 3 Ilmenite.

Reactions 1, 4, and 7 through 9 were used for high-grade gneisses without muscovite; reactions 1 through 6 were used for muscovite-bearing gneisses and schists.

The degree of consistency of the intersection among these equilibria may be considered a measure of the approach to equilibrium among the major components (Berman 1991). This is a

necessary condition from which to infer that the *P* and *T* of intersection are a precise estimate of the equilibration conditions for the assemblage. The lack of a consistent intersection, however, does not mean that all of the non-intersecting equilibria are not accurately recording *P* or *T*. Certain equilibria are more robust with regard to preservation of peak mineral compositions because of kinetic barriers to diffusion during falling temperature. For example, peak grossular content of garnet and anorthite content of plagioclase, related by net transfer equilibrium 4, can only be modified by resorption and recrystallization of garnet or plagioclase (see also Spear et al. 1991). During static retrograde cooling, resorption of garnet may in many cases be minimal and will not affect the equilibrium mass balance of Ca between plagioclase and garnet. However, resorption may be significant if retrograde cooling is accompanied by deformation. In contrast, Equilibrium 1 involves Fe-Mg exchange between garnet and biotite. The Fe and Mg diffuse more rapidly in garnet than does Ca (Chakraborty and Ganguly 1991, 1992), and much more rapidly in biotite than garnet (Spear 1989). Equilibrium 1 is thus very susceptible to continued volume diffusion and resetting of peak compositions during static cooling following peak conditions. This resetting may be exacerbated by garnet resorption reactions that release Fe and Mg components that exchange rapidly with matrix biotite, affecting the locus of reaction 1 (commonly resulting in anomalously high *T* estimates: Robinson et al. 1982; Spear 1991). Other equilibria are more sensitive to resetting due to a greater dependence of the equilibrium constant for the reaction on thermodynamic properties (generally a small ΔS and/or ΔV of reaction). These reactions magnify errors in activity-composition relations (Berman 1991) and errors associated with chemical analysis, and tend to be equilibria not involving anorthite component (reactions 5 and 6). Interpretation of the results of conventional thermobarometry requires consideration of all these factors in the context of the deformation and crystallization history of a metamorphic rock. The various samples analyzed here illustrate the range of possible outcomes of re-equilibration and resetting following a period of prograde metamorphism.

The accuracy of geothermobarometric calculations in general has been assessed elsewhere by propagation of errors (Hodges and McKenna 1987; Kohn and Spear 1991). Uncertainties in *P* and *T* depend on several factors (microprobe analytical precision, thermodynamic data, activity models, precision of experiments), and upon one another. Simple error propagation for this study found that uncertainties in garnet activity models (mainly grossular component) and temperature were most responsible for uncertainties in pressure. Microprobe analytical uncertainty [± 1 mol% Fe/(Fe + Mg) in biotite or garnet] has the greatest effect on temperature. For this study, analytical uncertainties for *T* and *P* are ± 50 °C and ± 1.5 kbar.

SAMPLE CHARACTERIZATION

Chemical and isotopic analyses were performed on metapelitic schists and gneisses with the assemblage Grt + Qtz + Bt + Ky/Sil \pm Pl \pm Ms \pm Kfs \pm Ilm \pm Ru from several settings in the Appalachian orogen of eastern North America (Pelham dome, Massachusetts; Willimantic window and Waterbury dome, Connecticut; southern Blue Ridge province, North Caro-

TABLE 4. Summary of mineral assemblages and important textural features

Sample no.	Field sample no.	Assemblage*	Important textural features
Pelham Dome			
1	PD947a-1 (schist)	Ms-Qtz-Bt-Pl-Grt-Ky-Str-Ilm	Single foliation; Ky + Str define lineation
2	PD947a-2 (gneiss)	Pl-Qtz-Sil-Kfs-Grt-Bt-Ru	Single (migmatitic) foliation
Waterbury Dome			
3	C90-23(fine-grained schist)	Qtz-Ms-Bt-Grt-Ky-Pl	Truncated Grt poikiloblasts; S1 foliation of Grt inclusions at angle to S2 matrix phases.
4	C90-23b (coarse-grained schist)	Grt-Qtz-Bt-Ms-Ky-Str-Ru	Grt porphyroblasts in weakly foliated Qtz-rich matrix
5	gsg92.9 (gneiss)	Bt-Ky-Ms-Grt-Qtz-Mc-Pl	Migmatitic S1 layering overprinted by S2 axial planar schistosity
6	rs92.3 (schist)	Bt-Ky-Grt-Qtz	Poorly foliated schist with resorbed garnet porphyroblasts
Willimantic Window			
7	C89-1 (gneiss)	Pl-Qtz-Sil-Kfs-Grt-Bt-Ru	Single (migmatitic) foliation
8	89-115 (schist)	Bt-Ky-Str-Grt-Ms-Pl-Qtz-Sil	Single foliation; Ky and Str include Grt; retro. Sil, Bt, and Ms
9	C90-14 (schist)	Bt-Ky-Ms-Qtz-Pl-Grt	Single foliation (aligned Bt, Ms, Ky) wrapping resorbed Grt
Southern Blue Ridge			
10	WSG93.1 (schist)	Grt-Sil-Bt-Kfs	Strong lineation (aligned Sil, Grt, Kfs)

* Mineral abbreviations after Kretz (1983).

lina). Details of the geology of these localities are presented in Robinson et al. (1992), Moecher and Wintsch (1994; also see Getty and Gromet 1992a), Dietsch (1989), and Absher and McSween (1985, 1986), respectively. The important structural and petrological characteristics of each locality and its samples are discussed below and summarized in Table 4.

Pelham dome

The Pelham dome is a low amplitude dome in central Massachusetts cored by Late Precambrian quartzofeldspathic gneisses, and structurally overlain by gneisses and schists metamorphosed during the Acadian (middle to late Devonian) orogeny (Robinson et al. 1992). We analyzed a sample of coarse-grained, migmatitic Acadian gneiss with the assemblage Kfs + Pl + Sil + Bt + Grt + Qtz + Ru (sample 2). The gneisses are inferred to be enclosed structurally within, and to have undergone reconstitution during the Alleghanian (Late Pennsylvanian to Permian) orogeny to medium-grained Ms + Qtz + Bt + Pl + Grt + Ky + Str + Ilm schist (sample 1; Robinson et al. 1992; Moecher 1999). Although reconstitution thoroughly reworked the margins of gneiss enclosed by schist, samples of gneiss unaffected by the reconstitution are preserved in outcrop. The gneiss and schist (samples 1 and 2, Table 1) each have undergone a single period of porphyroblast growth and fabric formation, albeit at different times.

Garnet in the gneiss and schist are compositionally homogeneous, except near the rim where retrograde diffusional exchange has resulted in a slight increase in Fe and decrease in Mg (Moecher 1999). All other phases are very homogeneous from grain to grain.

Waterbury dome

The Waterbury dome lies within the Connecticut Valley zone of western New England (Dietsch 1989). The dome is cored by migmatitic pelitic gneisses and schists, and granitic orthogneisses of probable Taconian age (Dietsch et al. 1998). We analyzed a fine-grained Ky + Bt + Kfs (microcline) + Grt + Pl + Ms + Qtz + Ru pelitic gneiss (sample 5) having a migmatitic compositional layering defined by biotite-rich and biotite-poor layers (Fig. 1a). These layers were folded into upright open folds with an axial planar foliation defined mainly by parallel-

ism of the (001) planes of biotite (F3 fold stage of Dietsch 1989). Very fine-grained garnet porphyroblasts are scattered throughout biotite-rich and biotite-poor layers consistent with garnet nucleation and growth at the time of formation of axial planar foliation.

A fine-grained pelitic schist (Bt + Ky + Ms + Qtz + Grt; sample 6) from the core of the Waterbury dome was also analyzed. The sample is biotite- and kyanite-rich, characterized by a weak foliation and compositional layering, and contains heavily resorbed garnet porphyroblasts that are usually seen breaking down to biotite ± kyanite (Fig. 1b).

Two textural modes of monazite extracted from the gneiss and schist analyzed here yield U-Pb ages of ca. 435 and 380 Ma (Dietsch et al. 1998), consistent with the interpretation based on textural evidence of a polymetamorphic history for the gneiss. The younger age, interpreted to be the time of F3 folding and foliation development, is concordant with ^{40}Ar - ^{39}Ar total fusion ages of 380–375 Ma for hornblende from amphibolite in the same outcrop as the sample of gneiss (Dietsch and Sutter 1987). This concordancy requires that the temperature attending F3 folding (and garnet growth in gneiss) was at or below the closure temperature for Ar diffusion in hornblende (500–550 °C; McDougall and Harrison 1988). This is an important constraint for assessing the results of conventional and oxygen isotope thermometry in this sample (discussed below).

The cover rocks of the Waterbury dome consist in part of The Straits Schist Formation, a graphitic schist containing the assemblage Ms + Qtz + Bt + Grt + Ky + Pl + Str + Ru + Ilm. Two textural components of the schist were analyzed, both from the same hand sample. The coarse-grained component (sample 4; Fig. 1c) contains subidioblastic garnet porphyroblasts, 7–15 mm in diameter, with inclusions of rutile and ilmenite; kyanite blades up to 2 cm in length with rutile inclusions in some cases; xenoblastic, lobate plagioclase grains up to 1 cm in the longest dimension; medium-grained, idioblastic, and inclusionless staurolite; and medium-grained biotite and muscovite.

Garnet in the coarse-grained component exhibits a prograde compositional zoning pattern with a core to rim decrease in Mn, Ca, and Fe, and an increase in Mg. The outer 100 µm exhibits a reversal of the zoning pattern, with a low-Mn “well” in which ilmenite and rutile inclusions are concentrated (Fig. 1c). The

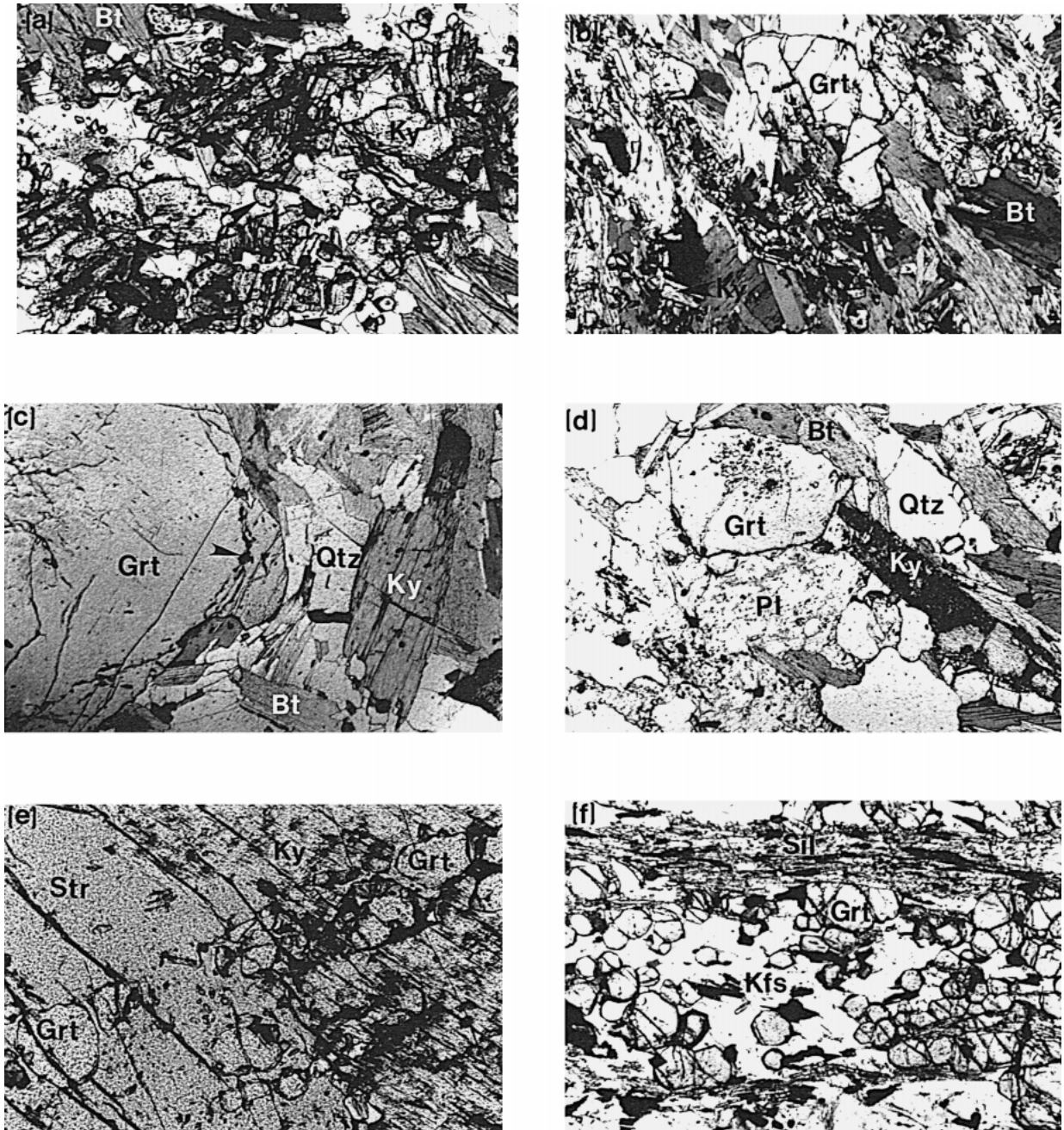


FIGURE 1. Photomicrographs illustrating mineral assemblages and important textural features used for interpretation of geothermometry. (a) Migmatitic pelitic gneiss from Waterbury dome (sample 5; horizontal field of view (fov) = 1.3 mm) with garnet (arrow heads), kyanite, potassium feldspar (clear) and biotite; orientation of (001) of biotite (upper left to lower right) defines F3 foliation, and compositional layering (upper right to lower left) defines earlier migmatitic layering; (b) schist (sample 6; fov = 4.1 mm) from Waterbury dome with resorbed garnet, kyanite (high relief granules), and biotite; (c) coarse-grained component of The Straits Schist (sample 4; fov = 9 mm) with large garnet (note dark ilmenite and rutile inclusions near margin of porphyroblast), kyanite, quartz, and biotite; (d) fine-grained component of The Straits Schist (sample 3c; fov = 4.1 mm) with resorbed garnet (note truncation of garnet by biotite), plagioclase, quartz, and kyanite (partially plucked during sample preparation); (e) inclusions of garnet in staurolite and kyanite in schist from Willimantic (sample 8; fov = 1.3 mm); (f) fine-grained sillimanite schist from Winding Stair Gap (sample 10; fov = 1.3 mm) with garnet, sillimanite, biotite (dark flakes) and potassium feldspar.

composition of garnet in the well was that used in conventional thermobarometric calculations. Plagioclase is compositionally variable and exhibits no consistent zoning pattern. The most sodic plagioclase composition obtained in each sample was used in thermobarometric calculations.

In contrast, a finer-grained component of the schist (sample 3; Fig. 1d) contains 2 mm, idio- to subidioblastic garnet with inclusion-rich (mainly quartz, biotite, and muscovite) cores, the inclusions exhibiting a preferred orientation at an angle to the present foliation, and inclusion-free, 100 to 300 μm wide rims. These garnets may be truncated by micas in the matrix, consistent with at least one period of matrix recrystallization following porphyroblast growth (Fig. 1d). Garnets are homogeneous with regard to major components, except for an increase in Fe and decrease in Mg in the outer 100 μm of the porphyroblast consistent with retrograde exchange with biotite (also see Miller et al. 1993; Lanzirotti 1995). The core composition of the fine-grained garnets is identical to that of the composition of the coarse-grained garnet "wells" in the same hand sample, suggesting that both types of garnet equilibrated at the same *P-T* conditions although they may have nucleated at different times and grown at different rates. Plagioclase is xenoblastic and tends to be reversely zoned (calcic rims, sodic cores), which is the opposite pattern predicted by models for prograde metamorphism in metapelites (Spear et al. 1991). The pattern is possibly due to resorption and incongruent dissolution of plagioclase with loss of albite component to muscovite during retrograde recrystallization, or to truncation of garnet and incorporation of what little grossular component was present in garnet.

Lanzirotti and Hanson (1995) carried out U-Pb geochronology on porphyroblast and matrix phases in The Straits Schist in the vicinity of the Waterbury dome. The Ky + Str grade metamorphism characteristic of The Straits Schist occurred at ~400 Ma. A later period of deformation and monazite growth occurred at 380–375 Ma, which is coincident with the time of open folding in the dome core (Dietsch et al. 1998; Sevigny and Hanson 1993). This two-stage history is supported by the textural evidence for a period of matrix recrystallization after porphyroblast growth.

Willimantic window

The Willimantic window exposes Late Precambrian gneisses beneath migmatitic rocks of Acadian age (400 Ma; Getty and Gromet 1992b) containing the assemblage Kfs + Pl + Qtz + Sil + Bt + Grt + Ru (sample 7; see Fig. 3 in Moecher and Wintsch 1994). The gneisses have undergone reconstitution in shear zones of inferred Alleghanian age (300–290 Ma; Getty and Gromet 1992b; Moecher and Wintsch 1994) to fine-grained schists containing the assemblage Bt + Ms + Pl + Qtz + Ky + Grt + Str. In some of these samples, coarse-grained kyanite and staurolite enclose fine-grained (500 μm in diameter) garnet porphyroblasts, suggesting garnet predates the enclosing phases (sample 8; Fig. 1e). The latter assemblages in turn, have experienced metamorphic overprinting during post-Alleghanian deformation. This overprinting is manifested either as a static Bt + Sil \pm Crd-grade overprint in some samples (sample 8 analyzed here; see Fig. 3 of Moecher and Wintsch 1994), or as

extensive recrystallization of the pre-existing Alleghanian fabric with resorption of garnet and rotation of kyanite into the plane of the foliation defined by biotite and muscovite (sample 9 analyzed here; see Fig. 4 of Moecher, in subm.). Additional details of mineral chemistry and compositional zoning of garnet in gneisses and schists from Willimantic are presented in Moecher and Wintsch (1994).

Southern Blue Ridge

Granulite facies pelitic rocks are exposed at Winding Stair Gap in western North Carolina (Absher and McSween 1985). Pelitic lithologies include migmatitic gneisses and fine-grained, strongly lineated, sillimanite- and garnet-rich schists. Based on orientation of various structural elements, melting occurred immediately following formation of the fabric in schist (Moecher 1998). Determination of temperatures of equilibration of the schist thus will provide an estimate of the melting temperature in the migmatite.

The schist (sample 10) is fine-grained and consists of idio- to subidioblastic garnet (0.5 mm in diameter) in a well-lineated matrix of acicular sillimanite, biotite, and perthitic potassium feldspar (Fig. 1f). Garnet is syn- to post-kinematic and homogeneous in composition, except for slight retrograde Fe-Mg zoning at garnet rims. Textural evidence is consistent with one period of deformation having produced the present fabric in the schist.

Numerous garnet porphyroblasts and biotite flakes in various textural modes were analyzed in two samples of schist for the purposes of conventional geothermometry. Garnet and biotite inclusions in Kfs were found to have the lowest and highest Fe contents, respectively, for each phase. Presumably, armoring of these phases by Kfs prevented retrograde Fe-Mg exchange between the two phases, thus preserving peak mineral compositions. The composition of included garnet and biotite was that used in conventional thermometry. Because the sample analyzed here lacks plagioclase and quartz, peak pressure was calculated from mineral compositions in interlayered gneisses and schist that contain plagioclase. The Qtz-Kfs isotopic fractionation (Bottinga and Javoy 1973) was used, with fractionations from Sharp (1995) to derive Kfs-Als and Kfs-Grt fractionations for the purposes of isotopic thermometry (Table 2).

RESULTS

Calculated temperatures based on oxygen isotope fractionations and conventional thermometry are presented in Table 1 and compared in a series of *P-T* plots (Figs. 2 through 7). The isotopic temperatures are depicted on each plot as vertical lines at the calculated temperature or vertical bars spanning the temperature range obtained from the Qtz-Als and Qtz-Grt oxygen isotope fractionations. Temperatures for the Als-Grt exchange are generally not plotted because of the temperature insensitivity of the Als-Grt fractionation.

Garnet-biotite temperature estimates for the Pelham gneiss (sample 2) are approximately 750 °C at 5–6 kbar (Fig. 2a). The Qtz-Grt and Qtz-Sil oxygen isotope temperatures are within analytical error of one another and are ~25 °C higher than garnet-biotite temperatures (Fig. 3). Isotopic temperatures for fraction-

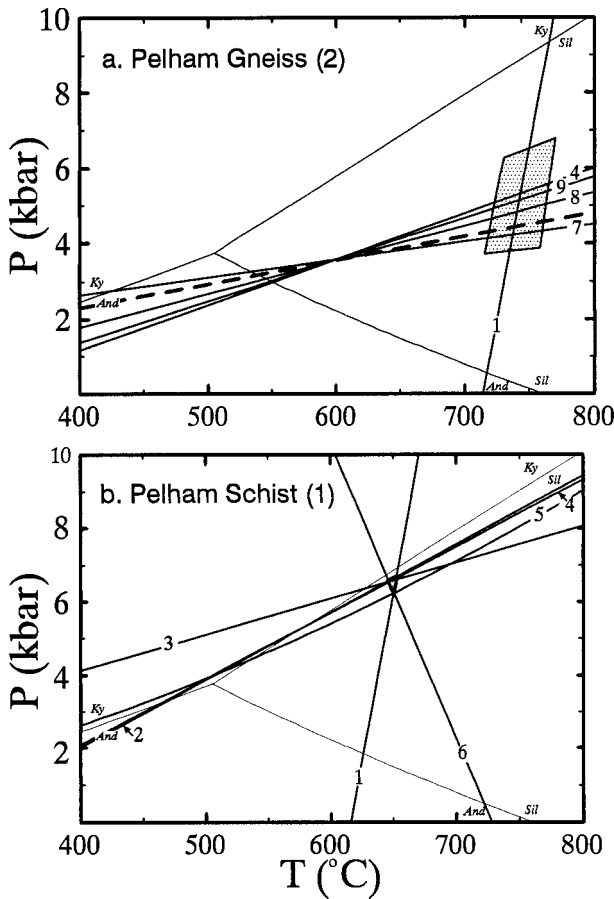


FIGURE 2. Examples of the results of conventional thermobarometry employing the TWEEQU approach of Berman (1991) for gneiss (a) and schist (b), Pelham dome. Numbered lines correspond to the P - T locus of reactions listed in the text. The intersection of equilibria 1-6 for schist is outlined by a small inverted triangle in b defined by independent Equilibria 1, 5, and 6. The shaded quadrilateral in a is an error box estimated from propagation of analytical uncertainty through geothermobarometric calculations (see text).

ations among Qtz, Ky, and Grt in the Pelham schist (sample 1) are identical to the temperature of intersection of Equilibria 1 through 6 (650 °C), the latter being a nearly perfect intersection for the mineral compositions used for geothermobarometry (Figs. 2b and 3).

Mineral equilibria for the coarse-grained component of the Straits Schist (sample 4) also define a very tight intersection at ~700 °C and 8-9 kbar; isotopic temperatures straddle this value (685 and 720 °C; Fig. 4). The temperature obtained using garnet core, the most sodic plagioclase, and matrix mica compositions in the fine-grained phase of schist (sample 3) is constrained less precisely, as shown by the dispersion of the intersection among equilibria 1 through 6 (Fig. 4). Temperature for the fine-grained schist component calculated using garnet rim, plagioclase rim and matrix mica compositions is considerably lower (~550 °C at 4 kbar), as are the temperatures based on Qtz-Ky and Qtz-Grt isotopic fractionations (574 and 585 °C) (Fig. 4).

The results for migmatitic pelitic gneiss from the core of

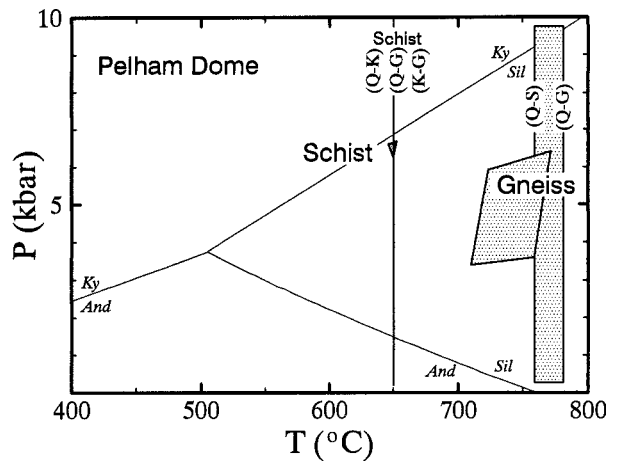


FIGURE 3. Comparison of conventional (small inverted triangle for schist, quadrilateral for gneiss) and isotopic thermometry (lines or shaded vertical bar) for Pelham Dome; Q-K, Q-S, Q-G, and K-G correspond to Qtz-Ky, Qtz-Sil, Qtz-Grt, and Ky-Grt temperatures based on oxygen isotope fractionations.

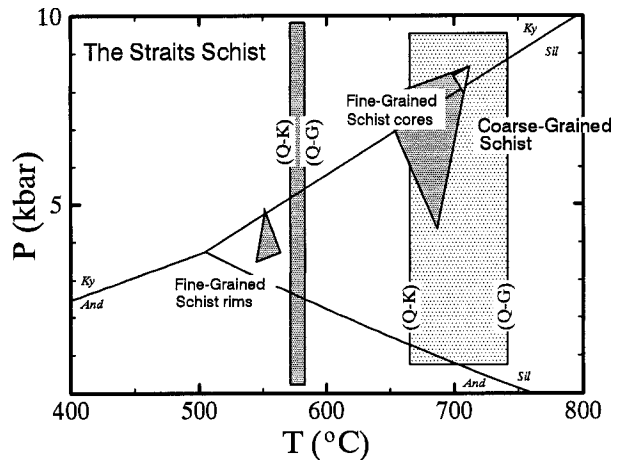


FIGURE 4. Results of conventional (triangles defined as in Fig. 3) and oxygen isotope thermometry (vertical bars) for fine- (dense stipple) and coarse-grained (light stipple) components of The Straits Schist. The intersection of equilibria 1, 4, and 7 through 9 for the coarse-grained component is the small inverted triangle coincident with the upper right corner of the triangle for the fine-grained component (larger densely stippled inverted triangle) using garnet and plagioclase core compositions.

the Waterbury dome (sample 5) are rather surprising. The Waterbury dome is the type locality for the Ky + Kfs + melt bathograd of Carmichael (1978), and phase equilibrium constraints require that kyanite + potassium feldspar be stable at high pressure and temperature relative to muscovite and quartz; the end-member reaction for pure phases occurs at approximately 800 °C at 8-9 kbar. However, the conventional thermobarometry for the sample of migmatitic gneiss defines a poor intersection at ~560 °C at 3-4 kbar (Fig. 5). Oxygen isotope thermometry is similarly low relative to the phase equilibrium constraints (540 and 570 °C for Qtz-Ky and Qtz-Grt fractionations). Conventional thermometry was not performed for the sample of schist

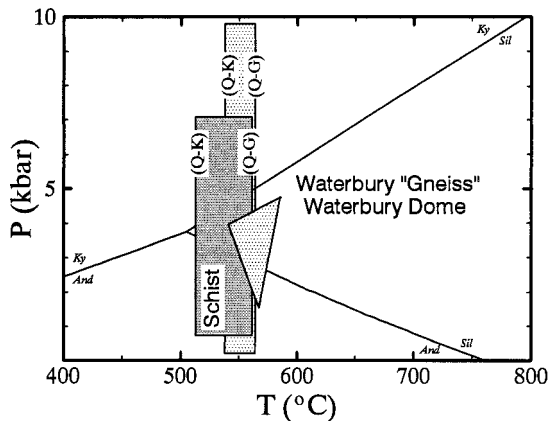


FIGURE 5. Results of conventional thermometry for migmatitic pelitic gneiss (sample 5; densely stippled triangle as in Fig. 3) and isotopic thermometry for gneiss and schist from the Waterbury dome.

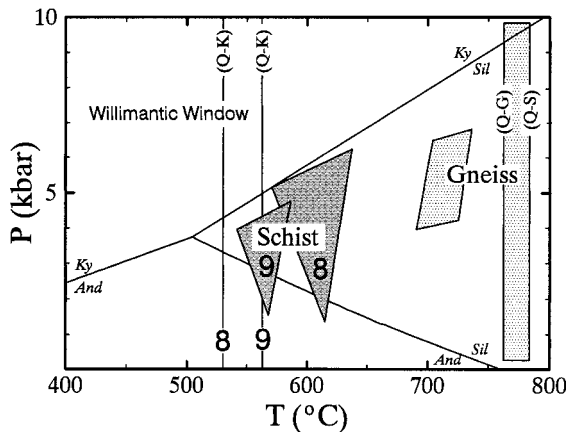


FIGURE 6. Results of conventional thermobarometry for migmatitic pelitic gneiss (light stipple) and schists (heavy stipple; samples 8 and 9) from the Willimantic Window.

(sample 6), in view of the extensive retrograde resorption of garnet and lack of plagioclase. Isotopic temperatures are 514 (Qtz-Ky) and 570 °C (Qtz-Grt) for the schist.

Conventional temperatures for migmatitic gneiss from the Willimantic window (sample 7) are slightly in excess of 700 °C at 5–6 kbar (Fig. 6), whereas isotopic temperatures are 760 and 780 °C (Qtz-Sil and Qtz-Grt, respectively). Samples of kyanite-bearing schist from the Willimantic window (sample 9) give the most unusual result for this study. Conventional geothermobarometry define a poor intersection for equilibria 1 through 6 in the temperature range 550–650 °C at 3–5 kbar (Fig. 6). Isotopic temperatures based on Qtz-Ky fractionations for both samples are ~550 °C. However, the kyanite-garnet fractionation for sample 9 is essentially zero, and that for sample 8 is negative, indicating a kyanite-garnet isotopic reversal (Table 1).

Isotopic temperatures from Kfs-Grt and Kfs-Sil fractionations for the sillimanite schist from the southern Blue Ridge (sample 10) are 855 and 840 °C, respectively, and the Sil-Grt temperatures are 814 °C (Fig. 7). In comparison, garnet-biotite thermometry for two samples of sillimanite schist yield tem-

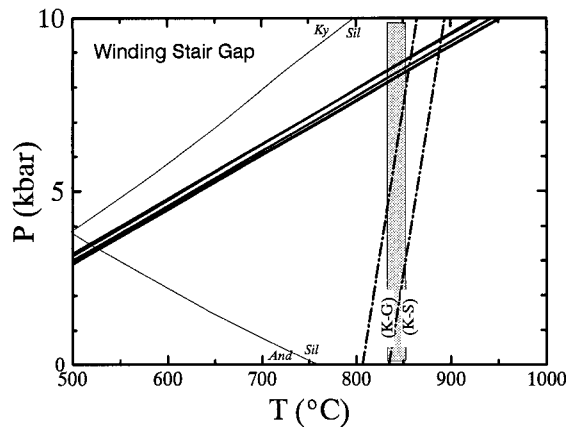


FIGURE 7. Results of isotopic and conventional schist (equilibrium 1 using garnet and biotite inclusions in Kfs, dash-dot lines) thermometry for sillimanite-rich from the southern Blue Ridge, and barometry (equilibrium 4) for migmatitic gneisses interlayered with schist (solid lines) from Moecher (1998).

peratures of 860 and 890 °C at 8–9 kbar, slightly higher than the isotopic temperatures. P - T conditions based on mineral compositions in plagioclase-bearing samples of schist and migmatite from Winding Stair Gap are 8–9 kbar at 850–900 °C (Fig. 7), based on Equilibria 1, 2, 4, and 7 through 9, and Hercynite-corundum-garnet-plagioclase-sillimanite equilibria in associated migmatites (Moecher 1998). These conditions are in good agreement with the isotopic temperatures and with peak conditions for various rock types in the area (~850–875 °C; Eckert et al. 1989; Tenthorpe et al. 1996).

DISCUSSION AND IMPLICATIONS

The results obtained in this study will be evaluated in the context of the metamorphic and deformation history of each sample, and in terms of hydrous vs. anhydrous retrograde oxygen isotope exchange among minerals. Some samples can be modeled in terms of a single period of metamorphism and preservation of peak temperatures. More complicated scenarios observed in our samples include closed-system retrograde recrystallization, closed-system retrograde recrystallization with re-equilibration, and open-system recrystallization with retrograde exchange (e.g., Hoffbauer et al. 1994).

The simplest case: A single period of metamorphism

Several samples (1–5, 10) yield conventional and isotopic temperatures that agree within error. The agreement may be accounted for in terms of major element and oxygen isotopic equilibrium being attained during, and preserved following, a single period of prograde metamorphism. The best possible agreement is obtained for the sample of Pelham schist (sample 2, Figs. 2 and 3), in which the relevant mineral equilibria intersect at essentially a single point, and all isotopic fractionations are concordant and agree with the temperature obtained from conventional equilibria. The common intersection indicates that the assumption of equilibrium phase compositions is valid. The agreement with isotopic temperatures indicates retrograde oxygen isotope exchange among minerals has been minimal or of

such a degree as to not affect the peak equilibrium isotopic compositions. The agreement is also evidence that the temperature obtained is accurate and represents that of peak metamorphism for this sample.

Internal consistency between isotopic and conventional exchange thermometry is not the norm for the samples analyzed here (discussed further below). It is possible that the exact concordance of the two thermometric approaches may be fortuitous and one of many random outcomes distributed about a mean of possible degrees of concordance. However several factors related to the history of the Pelham schist contribute to producing such an outcome. These include (1) a single period of fabric development and porphyroblast growth without significant garnet resorption and fabric modification following growth of porphyroblasts and crystallization of the matrix; (2) peak temperature not being excessively high so that retrograde garnet-biotite Fe-Mg exchange does not proceed to any significant extent; and (3) apparent cooling in the absence of a hydrous fluid phase (see below).

An inconsistency in the locus of the intersection for the sample of schist is that it falls just inside the sillimanite field. However, garnet in the schist is very low in grossular component ($X_{Gr} = 0.02$). An error of 0.01 mole percent grossular or in calculated activities, not unreasonable for garnets with such extreme compositions (Guiraud and Powell 1996), corresponds to an isothermal shift in equilibrium 4 of ± 1.5 kbar. Based on this effect, the imprecision in experimental location of the kyanite-sillimanite boundary (Newton 1966; Bohlen et al. 1991; also see Kerrick 1990), and the presence of abundant coarse-grained kyanite porphyroblasts, the sample is inferred to have equilibrated near the kyanite-sillimanite boundary but just in the kyanite field (7 kbar at 650 °C).

In order for quartz in the schist from Pelham to preserve its peak (650 °C) oxygen isotopic composition, modeling indicates that cooling had to be extremely rapid (in excess of 1000 °C/m.y.) or occurred in the absence of a hydrous fluid phase. Such an extreme cooling rate is completely unreasonable for a regional metamorphic terrane. Rather, use of anhydrous diffusion data for quartz and plagioclase in the model cooling calculations and a cooling rate of 10 °C/m.y. (a geologically reasonable rate for post-Alleghanian metamorphism in New England; Wintsch et al. 1993; Moecher 1999) reproduces within error the isotopic composition of quartz in the Pelham schist (Table 3). This does not imply that *prograde* metamorphism of the schist occurred under fluid-absent conditions. It merely indicates that a pervasive hydrous grain boundary fluid was not present during cooling (i.e., $a_{H_2O} < 1$). The absence of a hydrous fluid phase during cooling was inferred for granulite facies iron formation (Sharp et al. 1988 as discussed in Sharp 1991), pelitic schist (Massey et al. 1994), and ductilely deformed meta-anorthosite (Sharp and Moecher 1994). The important implication of this condition is that near-peak oxygen isotope compositions are retained by quartz, and that Qtz-Ky and Qtz-Grt fractionations may be used to retrieve peak metamorphic temperatures.

The degree of oxygen isotope equilibrium among phases in a rock is traditionally illustrated using a plot of $\Delta^{18}O_{(Qtz-Min)}$ vs. the temperature coefficient for fractionation ("A" in Eq. 1) (Javoy et al. 1970). In such a plot, all phases in isotopic equilibrium

must lie (within error) on a straight line—an isotherm—the slope of which is proportional to temperature. This condition is best exemplified by the Pelham schist, for which all isotopic fractionations yield concordant temperatures (Fig. 8). However, as will be shown below, all samples that lie along an isotherm are not necessarily in isotopic equilibrium (cf. Sharp and Moecher 1994).

Migmatitic Kfs+Sil gneiss from the Pelham dome (sample 1) and Willimantic window (sample 7) yield isotopic temperatures that are similar (probably because metamorphic grade is identical at both localities), yet slightly higher than those obtained from the garnet-biotite Fe-Mg exchange equilibrium (Figs. 2 and 5). These samples exhibit no evidence for retrograde mineral reactions such as the common hydration reaction resulting in resorption of garnet: almandine + potassium feldspar + water = sillimanite + biotite. The most likely explanation for conventional temperatures being lower than isotopic temperatures is retrograde Fe-Mg exchange between modally abundant garnet and much less abundant matrix biotite. This explanation is supported by the diffusional modification of garnet rims evident in microprobe traverses of garnet in gneiss from both localities (increase in Fe and decrease in Mg at constant Mn and Ca; Tracy 1982; Spear 1991).

Some degree of retrograde oxygen isotope exchange of quartz with biotite and feldspar might be expected, even under anhydrous conditions. The observed isotopic composition of quartz (13.9), although yielding fractionations corresponding to an apparent peak temperature of 775 °C, may have been lower at the peak of metamorphism. The $\delta^{18}O$ values of quartz, biotite, and feldspars were calculated at 825 °C and 850 °C based on the measured $\delta^{18}O$ for sillimanite. The observed (13.9 ± 0.1) and calculated (14.1 and 14.0) values for quartz in gneiss from Willimantic are within error for a peak temperature of 825–850 °C, respectively (anhydrous retrograde exchange), indicating quartz has undergone only slight resetting (Table 3). Similarly, the calculated isotopic composition of quartz in Pelham gneiss, for anhydrous cooling from an inferred peak T of 825–850 °C, is only slightly higher (0.1–0.2 per mil) than the observed value (Table 3). In both cases, the models predict

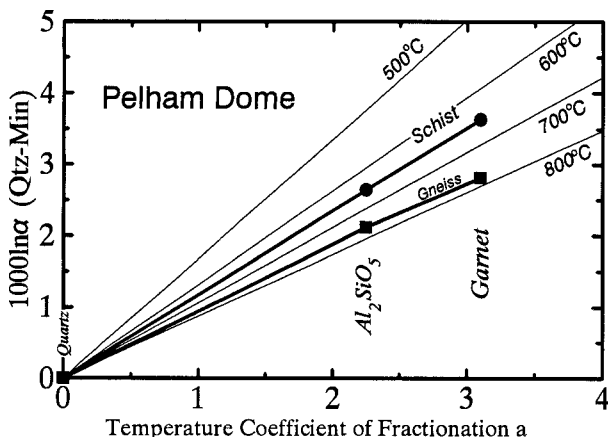


FIGURE 8. Isotherm plot (after Javoy et al. 1970) illustrating the approach to oxygen isotope equilibrium among quartz, aluminosilicates, and garnet in gneiss and schist from the Pelham dome.

greater degrees of retrograde exchange than is observed. This will be discussed further below.

There is general agreement between conventional and isotopic thermometry for other samples. The coarse-grained component of the Straits Schist (sample 4) exhibits a tight intersection among Equilibria 1, 4, and 7 through 9, within the kyanite field. The agreement between conventional and isotopic temperatures is good, and there was apparently minimal resetting of quartz isotopic compositions. The observed quartz values are consistent with anhydrous cooling from 700 °C (Table 3). The lack of resetting is, in this case, likely due to the coarse grain size of all phases (Table 3).

Garnet-biotite and oxygen isotope thermometry in sillimanite-rich schist from the Western Blue Ridge (sample 10) agree within error (875 and 840 °C, respectively). At such high temperatures, and even in the absence of a hydrous fluid phase during cooling, one might expect some degree of retrograde oxygen isotopic exchange between potassium feldspar and biotite. Thus, the $\Delta^{18}\text{O}_{\text{Kfs-Als}}$ and $\Delta^{18}\text{O}_{\text{Kfs-Grt}}$ are upper limits on peak values. Modeling the cooling history with an initial temperature of 900 °C and anhydrous conditions results in potassium feldspar compositions that are identical to the measured value (Table 3).

Closed-system recrystallization without reaction

The fine-grained component of The Straits Schist (sample 3) preserves evidence of a period of matrix recrystallization and fabric modification following porphyroblast growth that involved no apparent mineralogic reaction other than resorption of garnet. Resorbed garnet components should have been incorporated into micas, quartz, and plagioclase. In the absence of reaction or recrystallization, garnet and kyanite are unlikely to have undergone oxygen isotope re-equilibration with the matrix phases during recrystallization because of the extremely slow diffusion of oxygen in the former phases (Fortier and Giletti 1989; Young 1993). The minerals quartz-garnet-kyanite appear to be in mutual isotopic equilibrium at a temperature of 580 °C. This temperature is in good agreement with conventional estimates from the fine-grained rim compositions, but the agreement is fortuitous—the isotherm (Fig. 9) has no meaning (Giletti 1986; Sharp and Moecher 1994). The garnet and kyanite preserve their original $\delta^{18}\text{O}$ values from the peak metamorphic event, while the quartz re-equilibrated with other recrystallizing phases—biotite, muscovite, and plagioclase—during the period of deformation and crenulation formation 20 m.y. later. The garnet-kyanite fractionations correspond to 620 °C, in apparent agreement with Qtz-Grt and Qtz-Ky fractionations, but an uncertainty of only 0.1 per mil in the $\Delta^{18}\text{O}_{\text{Ky-Grt}}$ fractionations raises the temperature estimate to 700 °C—the temperature of the earlier event as inferred from sample 4.

The possibility of quartz re-equilibration may be evaluated by modeling oxygen isotope exchange during cooling. The proximity of the fine- and coarse-grained components (both from a 10 cm scale hand sample), the latter defining the prior high-temperature history for The Straits Schist (~700 °C at 8–9 kbar), requires that both components experienced the same thermal history. It is assumed that garnet, kyanite, and staurolite in all samples of The Straits Schist grew at ~400 Ma, the time of kya-

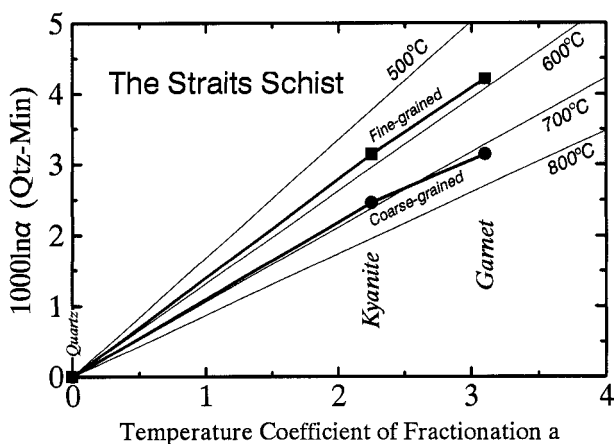


FIGURE 9. Isotherm plot for The Straits Schist. The fine-grained component yields an *apparent* isotherm that is argued to be the result of retrograde exchange of quartz with matrix micas and not equilibrium isotopic fractionation with kyanite and garnet.

nite and staurolite growth in The Straits Schist at the type locality (Lanzirotti and Hanson 1994). This Ky + Str-grade metamorphism was followed by a period of cooling (20 m.y.) from 700 to 550 °C, the latter being the temperature at which matrix phases in the fine-grained component recrystallized and re-equilibrated. This was followed by a period of cooling to the temperature of Ar closure in muscovite (~350 °C, McDougall and Harrison 1988) at 350 Ma (Dietsch and Sutter 1987).

Although there is structural, textural, and geochronologic evidence for a period of recrystallization at 380 Ma and 550 °C, in the absence of mineral reactions there is no way to incorporate explicitly a period of deformation into the thermal history. It is possible that such an episode has no bearing on retrograde isotopic exchange, other than to provide a short-term kinetic boost that aids in the exchange process. The thermal history was simply modeled as cooling from 700 °C to the closure temperature for the most rapid diffusing species under hydrous conditions.

The measured isotopic composition of quartz in the fine-grained schist is 0.3 and 0.6 per mil higher than modeled values for hydrous and anhydrous cooling, respectively (Table 3); i.e., quartz has re-equilibrated to a greater extent than predicted by simple diffusional exchange (assuming a closed system). This is the predicted effect for re-equilibration of quartz and micas during matrix recrystallization after garnet and kyanite growth. If matrix recrystallization and exchange of quartz and micas occurred, then Qtz-Ky and Qtz-Grt temperatures in this sample are merely apparent temperatures that fortuitously agree with thermochronologic constraints for the dome area. A test for recrystallization would be to analyze the micas as well, with modeling of the cooling history that followed recrystallization and exchange.

The argument for retrograde exchange may also be made for interpretation of conventional thermometry based on the composition of garnet rims in the fine-grained schist. Garnets with diameters of 1–2 mm in this sample exhibit the typical pattern of constant Fe and Mg concentration through their cores with increasing Fe/(Fe+Mg) near the rim, interpreted as ho-

mogenization by volume diffusion at high temperature followed by retrograde Fe-Mg exchange with biotite. Empirical evidence and modeling have shown (Spear 1991) that retrograde Fe-Mg diffusion will tend to yield garnet rim-matrix biotite temperatures between 450 and 550 °C, and that this temperature cannot be assigned to a specific geologic event. The time at which the closure temperature was attained for diffusion of Fe and Mg in garnet fortuitously coincided with a period of regional deformation. Likewise, use of garnet core and matrix biotite compositions in conventional thermometry is inappropriate because of garnet resorption, unless the modal amount of resorption was insignificant compared to that of biotite.

Closed-system recrystallization with re-equilibration

The sample of migmatitic Waterbury gneiss clearly has a complex metamorphic history, which is supported by textural observations and geochronology. An early high-grade (Ky + Kfs-grade) metamorphism was followed by folding and recrystallization, manifested in formation of an axial planar foliation along with nucleation of monazite and garnet. The temperature of this event is independently constrained from thermochronology to be ~550 °C, which agrees well with the Qtz-Ky and Qtz-Grt isotopic temperatures and conventional geothermobarometry for this sample (Fig. 5). Isotopic compositions of quartz, kyanite, and garnet in this sample define an isotherm (Fig. 10). Questions regarding the interpretation of the oxygen isotope systematics of this sample are similar to those for the fine-grained component of the Straits Schist: what is the timing of kyanite and garnet formation relative to matrix phases; are the observed Qtz-Ky and Qtz-Grt fractionations equilibrium values established via mineral reactions at 380 Ma and 550 °C; and, to what extent have the Qtz-Ky and Qtz-Grt fractionations been reset by exchange of fine-grained quartz with other matrix phases (mainly biotite)?

Garnet occurs as very fine-grained equant inclusions in all minerals in the migmatitic gneiss, and appears to have nucleated randomly throughout the sample; fine-grained kyanite is concentrated in aggregates scattered throughout the sample (Fig.

1a). In the absence of U-Pb ages on garnet and kyanite, or Sm-Nd mineral isochrons, there is no compelling textural evidence to discount the assumption that garnet formed and kyanite recrystallized during the most recent period of crenulation development. Quartz and microcline probably recrystallized, given their documented tendency to do so during deformation. Micas defining the present foliation may have been partly rotated into parallelism, but based on the results of modeling discussed above they were probably open to exchange by volume diffusion of O, Mg, and Fe during recrystallization of other phases.

The cooling history of the gneiss was simulated to determine the isotopic composition of quartz given equilibration with garnet and kyanite at 550 °C. Modeled quartz isotopic compositions are slightly greater than, but within error of, the measured value (Table 3). Quartz appears to have “closed” to oxygen diffusion sooner than predicted by the models, similar to the samples of gneiss described above. If these discrepancies were due to random error in input parameters, we would expect some modeled quartz isotopic compositions to be less than observed values. For the samples we analyzed, this is the case only for the fine-grained Straits Schist discussed above. The overestimation of the extent of exchange may reflect use of hydrous mica diffusion data. Diffusion parameters for micas under hydrous conditions are of similar magnitude as for quartz and feldspars. If these parameters are of similar magnitude in biotite as in quartz and feldspars under anhydrous conditions, then very little if any retrograde diffusive exchange would be expected for quartz in mica-bearing rocks.

Modeling supports the interpretation that kyanite and garnet grew in this sample during the younger, lower temperature phase of metamorphism in the Waterbury dome area. If 750 °C was the temperature at which kyanite, garnet, and quartz last equilibrated (consistent with conditions needed for melting in the Waterbury gneiss; Li 1994), and kyanite preserves its peak isotopic composition, then the observed isotopic composition of quartz should be 13.0 per mil. The measured value is 13.5 per mil.

Open-system recrystallization with retrograde reactions

A very unusual result was obtained for both samples of variably sheared and partly retrograded kyanite-grade schist from the Willimantic dome: isotopic reversals and disequilibrium involving garnet and kyanite (Fig. 11). Garnet was found to possess an oxygen isotopic composition that was either greater than or the same as kyanite. The effects are present in both samples, which are texturally distinct and no less than 10 m apart in outcrop; similar results were obtained on a sample of ductilely deformed Grt-Kfs-Qtz-Ru gneiss from the Snowbird tectonic zone of northern Saskatchewan, Canada (Hanmer et al. 1995; Snoeyenboss 1997; included here for the purposes of comparison only) (Tables 1 and 4).

Inclusions of fine-grained garnet in coarse-grained kyanite and staurolite indicate that kyanite grew after garnet in sample 8 (Fig. 1e). Kyanite grains in sample 9 occur in a fine-grained, well-foliated matrix of biotite + muscovite + plagioclase + quartz + potassium feldspar, with the foliation being deflected around partly resorbed garnet porphyroclasts. Both textures support the interpretation that kyanite and quartz nucleated and recrystallized after formation of garnet. The most likely mecha-

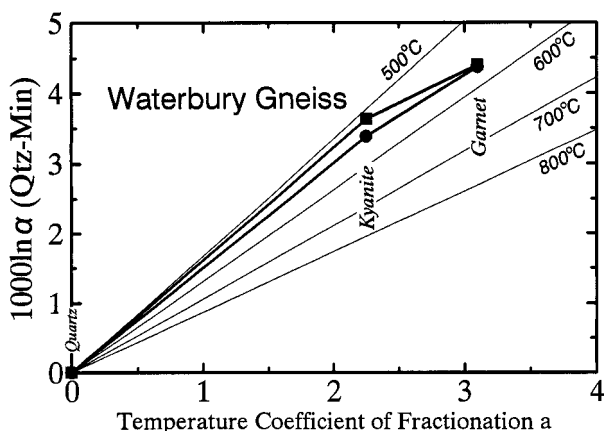


FIGURE 10. Isotherm plot for migmatitic pelitic gneiss (circles) and schist (squares) from the core of the Waterbury dome. Isotopic disequilibrium in schist is indicated by the nonlinearity of fractionations among garnet, kyanite, and quartz.

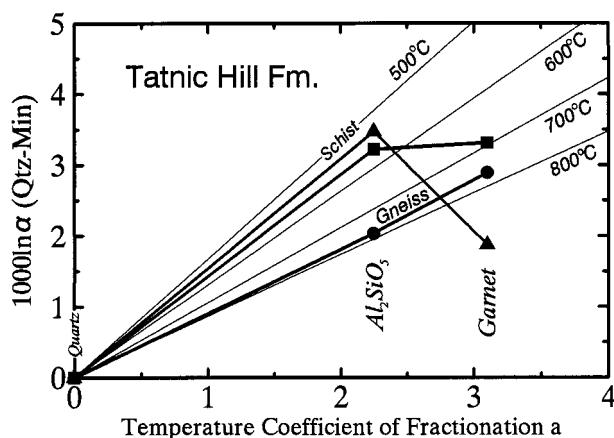


FIGURE 11. Isotherm plot for Willimantic gneiss and schists (squares = sample 8; triangles = sample 9) illustrating isotopic disequilibrium between quartz and garnet, and isotopic reversals between kyanite and garnet.

nism for producing the observed pattern of isotopic values is open-system kyanite-grade metamorphism and garnet resorption, where newly formed kyanite, staurolite, and matrix phases exchanged with an isotopically light fluid thus lowering the bulk isotopic composition of the rock. Although garnet reacted (in the sense that garnet components released during resorption were consumed by newly formed minerals), garnet did not exchange via volume diffusion and equilibrate with the kyanite and matrix phases, but it preserved $\delta^{18}\text{O}$ values of a higher-temperature event. In contrast, kyanite and quartz crystallized—in equilibrium—at $\sim 500\text{--}600^\circ\text{C}$.

As growth of kyanite (\pm staurolite) was the most recent mineral-forming event, the thermal history of the Willimantic schists was modeled to reproduce the observed isotopic composition of quartz. It was found that hydrous cooling from 600°C exactly reproduces the quartz values for sample 8, although anhydrous cooling from 550°C cannot be discounted. Anhydrous cooling from 600°C exactly reproduces values for sample 9, although the value for cooling starting at 550°C is within error of the observed value (Table 3).

If garnet grew during a previous period of metamorphism, then conventional geothermobarometry in these samples is likely to yield inconsistent results as well (Fig. 6). Moecher and Wintsch (1994) performed such analysis for the Ky + Str-grade rocks at Willimantic based on equilibria involving garnet. The lack of consistent results among thermobarometers and rationalizations for justifying their applicability made it clear at the time that not all minerals were in major-element equilibrium. However, it may be possible to extract estimates of P and T based on equilibria that are difficult to reset during subsequent periods of metamorphism, e.g., the garnet-plagioclase-aluminosilicate-quartz thermobarometer. Alternatively, one may have to rely on constraints from phase equilibria or petrogenetic grids to reconstruct the P - T history of such complex rocks.

Schist from the core of the Waterbury dome (sample 6) exhibits what could be interpreted as open-system retrograde reaction. Garnet, kyanite, and quartz do not define an isotherm (Fig. 10), although the degree of nonlinearity is not as marked

as it is for the Willimantic schists. Textural evidence for resorption of garnet and formation of biotite, kyanite, and quartz is consistent with operation of the reaction $\text{Kfs} + \text{Grt} + \text{H}_2\text{O} = \text{Ky} + \text{Bt} + \text{Qtz}$, which requires a source of hydrating fluid. It is most likely that kyanite and quartz are in isotopic equilibrium, as they formed contemporaneously.

SUMMARY

Careful consideration of the reaction history and textural evolution of metamorphic rocks permit very precise and accurate constraints on their thermal evolution to be derived from oxygen isotope fractionations among refractory minerals such as kyanite and garnet combined with conventional thermometry. Stable isotope thermometry may in specific cases be in excellent agreement with temperature constraints derived from conventional thermobarometry. This is most likely to occur in metamorphic rocks with a simple prograde metamorphic history, for which cooling occurred in the absence of a hydrous fluid phase, or for sub-granulite facies settings. Stable isotope fractionations, in the absence of a hydrous fluid, are likely to provide more accurate constraints on peak temperature in granulite facies settings than are cation exchange equilibria (also see Farquhar et al. 1996). It is evident that application of stable isotope thermometry is subject to the same caveats as conventional thermometry, particularly in high grade or polymetamorphic metapelitic rocks (Spear 1991; Eiler et al. 1993; Farquhar et al. 1993). Considerations need to be made for isotopic mass balance, diffusional effects, and reaction histories. Thermometric constraints possessing geologic significance are in some cases retrievable. In other cases, however, both isotopic and conventional temperatures are at best minimum estimates of peak temperature and correspond to some stage in the cooling history that cannot be ascribed to a specific event or whose age cannot be constrained by thermochronology.

ACKNOWLEDGMENTS

We appreciate the constructive reviews of Jim Farquhar and John Eiler. Eiler is thanked for providing a copy of FGB. Mike Williams and Dave Snoeyenboss provided the gneiss from Saskatchewan. This research was supported in part by a Research Committee Grant from the University of Kentucky.

REFERENCES CITED

- Absher, B.S. and McSween, H.Y. Jr. (1985) Granulites at Winding Stair Gap, North Carolina: The thermal axis of Paleozoic metamorphism in the southern Appalachians. *Geological Society of America Bulletin*, 96, 588–599.
- Berman, R.G. (1988) Internally-consistent thermodynamic data for minerals in the system $\text{Na}_2\text{O-K}_2\text{O-CaO-MgO-FeO-Fe}_2\text{O}_3\text{-Al}_2\text{O}_3\text{-SiO}_2\text{-TiO}_2\text{-H}_2\text{O-CO}_2$. *Journal of Petrology*, 29, 445–522.
- (1990) Mixing properties of Ca-Mg-Fe-Mn garnets. *American Mineralogist*, 75, 328–344.
- (1991) Thermobarometry using multi-equilibrium calculations: A new technique, with petrological applications. *Canadian Mineralogist*, 29, 833–855.
- Bohlen, S.R., Montana, A., and Kerrick, D.M. (1991) Precise determinations of the equilibria kyanite = sillimanite and kyanite = andalusite and a revised triple point for Al_2SiO_5 polymorphs. *American Mineralogist*, 76, 677–680.
- Bottinga, Y. and Javoy, M. (1973) Oxygen isotope partitioning among minerals in igneous and metamorphic rocks. *Reviews of Geophysics and Space Physics*, 13, 401–418.
- Bowman, J.R. and Ghent, E.D. (1986) Oxygen and hydrogen isotope study of minerals from metapelitic rocks, staurolite to sillimanite zones, Mica Creek, British Columbia. *Journal of Metamorphic Geology*, 4, 131–141.
- Carmichael, D.M. (1978) Metamorphic bathozones and bathograds: A measure of the depth of post-metamorphic uplift and erosion on the regional scale. *American Journal of Science*, 278, 769–797.
- Chacko, T., Hu, X., Mayeda, T.K., Clayton, R.N., and Goldsmith, J.R. (1996) Oxy-

- gen isotope fractionations in muscovite, phlogopite, and rutile. *Geochimica et Cosmochimica Acta*, 60, 2595–2608.
- Chakraborty, S. and Ganguly, J., (1991) Compositional zoning and cation diffusion in garnets. In, Ganguly, J., Ed., *Diffusion, Atomic Ordering, and Mass Transport*. *Advances in Physical Geochemistry*, v. 8, 120–175. Springer-Verlag, New York.
- (1992) Cation diffusion in aluminosilicate garnets: experimental determination in spessartine-almandine diffusion couples, evaluation of effective binary diffusion coefficients, and applications: *Contributions to Mineralogy and Petrology*, 111, 74–86.
- Chamberlain, C.P., Ferry, J.M., and Rumble III, D. (1990) The effect of net-transfer reactions on the isotopic composition of minerals. *Contributions to Mineralogy and Petrology*, 105, 322–336.
- Clayton, R.N. and Epstein, S. (1961) The use of oxygen isotopes in high-temperature geological thermometry. *Journal of Geology*, 68, 447–452.
- Clayton, R.N., Goldsmith, J.R., and Mayeda, T.K. (1989) Oxygen isotope fractionation in quartz, albite, anorthite, and calcite. *Geochimica et Cosmochimica Acta*, 53, 725–733.
- Dietsch, C. (1989) The Waterbury Dome, west central Connecticut: a triple window exposing deeply deformed, multiple tectonic units. *American Journal of Science*, 289, 1070–1097.
- Dietsch, C. and Sutter, J.R. (1987) Tectonic and metamorphic evolution of western Connecticut as interpreted from $^{40}\text{Ar}/^{39}\text{Ar}$ data. *Geological Society of America Abstracts with Programs*, 19, 11.
- Dietsch, C., Lanzirrotti, A., and Moecher, D.P. (1998) U-Pb, oxygen isotope, and petrologic constraints on the tectonothermal evolution of the Waterbury dome, Connecticut Valley belt, western New England. *Geological Society of America Abstracts with Programs*, 30, 14.
- Donovan, J.J., Rivers, M.L., and Armstrong, J.T. (1991) PRSUPR; automation and analysis software for wavelength dispersive electron-beam microanalysis on a PC. *American Mineralogist*, 77, 444–445.
- Eckert, J.O., Hatcher, R.D., and Mohr, D.W. (1989) The Wayah granulite-facies metamorphic core, southwestern North Carolina: High-grade culmination of Taconic metamorphism in the southern Blue Ridge. *Geological Society of America Bulletin*, 101, 1434–1447.
- Eiler, J.M., Baumgartner, L.P., and Valley, J.W. (1992) Interdiffusion of stable isotopes: A fast grain boundary model. *Contributions to Mineralogy and Petrology*, 112, 543–557.
- Eiler, J.M., Valley, J.W., and Baumgartner, L.P. (1993) A new look at stable isotope thermometry. *Geochimica et Cosmochimica Acta*, 57, 2571–2583.
- Eiler, J.M., Baumgartner, L.P., and Valley, J.W. (1994) Fast Grain Boundary: a FORTRAN-77 program for calculating the effects of retrograde interdiffusion of stable isotopes. *Computers and Geosciences*, 20, 1415–1434.
- Elphick, S.C., Graham, C.M., and Dennis, P.F. (1988) An ion microprobe study of anhydrous oxygen diffusion in anorthite: A comparison with hydrothermal data and some geological implications. *Contributions to Mineralogy and Petrology*, 100, 490–495.
- England, P.C. and Thompson, A.B. (1984) Pressure-temperature-time paths of regional metamorphism: I. Heat transfer during the evolution of regions of thickened continental crust. *Journal of Petrology*, 25, 894–928.
- Farquhar, J., Chacko, T., and Frost, B.R. (1993) Strategies for high temperature oxygen isotope thermometry: a worked example from the Laramie Anorthosite complex, Wyoming USA. *Earth and Planetary Science Letters*, 117, 407–422.
- Farquhar, J., Chacko, T., and Ellis, D.J. (1996) Preservation of oxygen isotope compositions in granulites from Northwestern Canada and Enderby Land, Antarctica: implications for high-temperature isotopic thermometry. *Contributions to Mineralogy and Petrology*, 125, 213–224.
- Fortier, S.M. and Giletti, B.J. (1989) An empirical model for predicting diffusion coefficients in silicate minerals. *Science*, 245, 1481–1484.
- (1991) Volume self diffusion of oxygen in biotite, muscovite, and phlogopite micas. *Geochimica et Cosmochimica Acta*, 55, 1319–1330.
- Getty, S.R. and Gromet, L.P. (1992a) Evidence for extension at the Willimantic Dome, Connecticut; implications for the late Paleozoic tectonic evolution of the New England Appalachians. *American Journal of Science*, 292, 398–420.
- (1992b) Geochronological constraints on ductile deformation, crustal extension, and doming about a basement-cover contact, New England Appalachians. *American Journal of Science*, 292, 359–397.
- Ghent, E.D. and Valley, J.W. (1998) Oxygen isotope study of quartz- Al_2SiO_5 -pairs from the Mica Creek area, British Columbia; implications for the recovery of peak metamorphic temperatures. *Journal of Metamorphic Geology*, 16, 223–230.
- Giletti, B.J. (1986) Diffusion effects on oxygen isotope temperatures of slowly cooled igneous and metamorphic rocks. *Earth and Planetary Science Letters*, 77, 218–228.
- Giletti, B.J. and Yund, R.A. (1984) Oxygen diffusion in quartz. *Journal of Geophysical Research*, 89, 4039–4046.
- Gillette, B.J., Semet, M.P., and Yund, R.A. (1978) Studies in diffusion. III. Oxygen in feldspars, an ion microprobe determination. *Geochimica et Cosmochimica Acta*, 42, 45–57.
- Guiraud, M. and Powell, R. (1996) How well known are the thermodynamics of Fe-Mg-Ca garnet? Evidence from experimentally determined exchange equilibria. *Journal of Metamorphic Geology*, 14, 75–84.
- Hanmer, S., Williams, M., and Kopf, C. (1995) Striding-Athabasca mylonite zone: implications for the Archean and Early Proterozoic tectonics of the western Canadian Shield. *Canadian Journal of Earth Sciences*, 32, 178–196.
- Hodges, K.V. and McKenna, L.W. (1987) Realistic propagation of uncertainties in geologic thermobarometry. *American Mineralogist*, 72, 671–680.
- Hoffbauer, R., Hoernes, S., and Fiorentini, E. (1994) Oxygen isotope thermometry based on a refined increment method and its applications to granulite-grade rocks from Sri Lanka: *Precambrian Research*, 66, 199–220.
- Holland, T.J.B. and Powell, R. (1990) An enlarged and updated internally consistent thermodynamic dataset with uncertainties and correlations: the system $\text{K}_2\text{O}-\text{Na}_2\text{O}-\text{CaO}-\text{MgO}-\text{MnO}-\text{FeO}-\text{Fe}_2\text{O}_3-\text{Al}_2\text{O}_3-\text{SiO}_2-\text{TiO}_2-\text{C}-\text{H}_2-\text{O}_2$. *Journal of Metamorphic Geology*, 8, 89–124.
- Javoy, M., Fourcade, S., and Allegre, C.J. (1970) Graphical method for examination of $^{18}\text{O}/^{16}\text{O}$ fractionations in silicate rocks. *Earth and Planetary Science Letters*, 10, 12–16.
- Jenkin, G.R.T., Fallick, A.E., Farrow, C.M., and Bowes, G.E. (1991) COOL: a FORTRAN-77 computer program for modeling stable isotopes in cooling closed systems. *Computers and Geoscience*, 17, 391–412.
- Jenkin, G.R.T., Farrow, C.M., Fallick, A.E., and Bowes, G.E. (1994) Oxygen isotope exchange and closure temperatures in cooling rocks. *Journal of Metamorphic Geology*, 12, 221–235.
- Kerrick, D.M. (1990) The Al_2SiO_5 polymorphs. In *Mineralogical Society of America Reviews in Mineralogy*, 22, 360.
- Kieffer, S.W. (1982) Thermodynamics and lattice vibrations of minerals: 5. Applications to phase equilibria, isotopic fractionations, and high pressure thermodynamic properties. *Reviews in Geophysics and Space Physics*, 20, 827–849.
- Kohn, M.J. (1993) Modeling prograde mineral $\delta^{18}\text{O}$ changes in metamorphic systems. *Contributions to Mineralogy and Petrology*, 113, 249–261.
- Kohn, M.J. and Spear, F.S. (1991) Error propagation for barometers. 2. Application to natural rocks. *American Mineralogist*, 76, 138–147.
- Kretz, R. (1983) Symbols for rock-forming minerals. *American Mineralogist*, 68, 277–279.
- Lanzirrotti, A. (1995) Yttrium zoning in metamorphic garnets. *Geochimica et Cosmochimica Acta*, 59, 4105–4110.
- Lanzirrotti, A. and Hanson, G.N. (1995) U-Pb dating of major and accessory minerals formed during metamorphism and deformation of metapelites. *Geochimica et Cosmochimica Acta*, 59, 2513–2526.
- Li, P. (1993) A petrological and origin study of layered migmatitic rocks in the Waterbury dome, Waterbury, CT: unpublished M.S. thesis, University of Cincinnati, 247 p.
- Massey, J.A., Harmon, R.S., and Harris, N.B.W. (1994) Contrasting retrograde oxygen isotope exchange behavior and implications: examples from the Langtang Valley, Nepal. *Journal of Metamorphic Geology*, 12, 261–272.
- McDougall, I. and Harrison, T.M. (1988) *Geochronology and Thermochronology by the $^{40}\text{Ar}/^{39}\text{Ar}$ Method*. Oxford University Press, New York, 212 p.
- Miller, S.J., Armstrong, T.R., and Tracy, R.J. (1993) Thermobarometric constraints on Acadian tectonic evolution in western Connecticut. *Geological Society of America Abstracts with Programs*, 25, A-423.
- Moecher, D.P. (1998) Kyanite-sillimanite-melt relations at Winding Stair Gap, NC: A re-evaluation of an alternative view. *Geological Society of America Abstracts with Programs*, v. 30, no. 4, 52.
- Moecher, D.P. (1999) The distribution, style, and intensity of Alleghanian Metamorphism in south-central New England: Petrologic evidence from the Pelham and Willimantic domes. *Journal of Geology*, in press.
- Moecher, D.P. and Wintsch, R.P. (1994) Deformation-induced reconstitution and local resetting of mineral equilibria in polymetamorphic gneisses: tectonic and metamorphic implications. *Journal of Metamorphic Petrology*, 12, 523–538.
- Newton, R.C. (1966) Kyanite-sillimanite equilibrium at 750°C. *Science*, 151, 1222–1225.
- O'Neil, J.R. and Clayton, R.N. (1964) Oxygen isotope thermometry. In H. Craig, S.L. Miller, and G.J. Wasserburg, Eds., *Isotopic and Cosmic Chemistry*, 157–168. North Holland Publishing, Amsterdam.
- Robinson, P.R., Holochoer, K.T., Tracy, R.J., and Dietsch, C.W. (1982) High grade Acadian regional metamorphism in south-central Massachusetts. In R. Joesten and S. Quarrier, Eds., *NEIGC 77th Annual Meeting*, Storrs, CT, 289–340.
- Robinson, P., Tucker, R.D., Gromet, L.P., Ashendon, D.D., Williams, M.L., Reed, R., and Peterson, V.L. (1992) The Pelham dome, central Massachusetts: Stratigraphy, geochronology, structure, and metamorphism. In P. Robinson and J.B. Brady, Eds., *Guidebook for Field Trips in the Connecticut Valley Region of Massachusetts and Adjacent States*, NEIGC 84th Annual Meeting: University of Massachusetts, Department of Geology and Geography Contribution No. 66, 132–169.
- Sevigny, J.H. and Hanson, G.N. (1993) Orogenic evolution of the New England Appalachians of southwestern Connecticut. *Geological Society of America Bulletin*, 105, 1591–1605.
- Sharp, Z.D. (1995) Oxygen isotope geochemistry of the Al_2SiO_5 polymorphs. *American Journal of Science*, 295, 1058–1076.
- Sharp, Z.D. and Moecher, D.P. (1994) O-isotope variations in a porphyroclastic

- meta-anorthosite: Diffusion effects and false isotherms. *American Mineralogist*, 79, 951–959.
- Sharp, Z.D., O'Neil, J.R., and Essene, E.J. (1988) Oxygen isotope variations in a granulite-grade iron formation: Constraints on oxygen diffusion and retrograde isotopic exchange. *Contributions to Mineralogy and Petrology*, 98, 490–501.
- Sharp, Z.D., Giletti, B.J., and Yoder, H.S. Jr. (1991) Oxygen diffusion rates in quartz exchanged with CO₂. *Earth and Planetary Science Letters*, 107, 339–348.
- Snoeyenbos, D.R. (1997) Archean high pressure metamorphism in the Snowbird Tectonic Zone, northern Saskatchewan. *Geological Association of Canada - Mineralogical Association of Canada Abstracts*, 22, A-140.
- Spear, F.S. (1989) Petrologic determination of metamorphic pressure-temperature-time paths. In Spear, F.S., and Peacock, S.M., Eds., *Metamorphic Pressure-Temperature-Time Paths*. American Geophysical Union Short Course in Geology, 7, 1–55.
- Spear, F.S. (1991) On the interpretation of peak metamorphic temperatures in light of garnet diffusion during cooling. *Journal of Metamorphic Geology*, 9, 379–388.
- Spear, F.S. and Florence, F.P. (1992) Thermobarometry in granulites: pitfalls and new approaches. *Precambrian Research*, 55, 209–241.
- Spear, F.S., Kohn, M.J., Florence, F.P., and Menard, T. (1991) A model for garnet and plagioclase growth in pelitic schists: implications for thermobarometry and P-T path determinations. *Journal of Metamorphic Geology*, 8, 683–696.
- Tenthorey, E.A., Ryan, J.G., and Snow, E.A. (1996) Petrogenesis of sapphirine-bearing metatrololites from the Buck Creek ultramafic body, southern Appalachians. *Journal of Metamorphic Geology*, 14, 103–114.
- Tracy, R.J. (1982) Compositional zoning and inclusions in metamorphic minerals. In *Mineralogical Society of America Reviews in Mineralogy*, 10, 355–397.
- Valley, J.W., Chiarenzelli, J.R., and McLelland, J.M. (1994) Oxygen isotope geochemistry of zircon. *Earth and Planetary Science Letters*, 126, 187–206.
- Wintsch, R.P., Sutter, J.F., Kunk, M.J., Aleinikoff, J.N., and Boyd, J.L. (1993) Alleghanian assembly of Proterozoic and Paleozoic lithotectonic terranes in south central New England: New constraints from geochronology and petrology. In J.T. Cheney and T.C. Hepburn, Eds., *Field trip guidebook for the north-eastern United States: Amherst, Massachusetts*, Geology Department, University of Massachusetts, Contribution 67, v. 1, H1–H30.
- Young, E.D. (1993) On the ¹⁸O/¹⁶O record of reaction progress in open and closed metamorphic systems. *Earth and Planetary Science Letters*, 117, 147–167.

MANUSCRIPT RECEIVED APRIL 6, 1998

MANUSCRIPT ACCEPTED APRIL 22, 1999

PAPER HANDLED BY PETER I. NABELEK

APPENDIX TABLE 1. Electron microprobe analyses

	Biotite						Muscovite			
	C90-23a	C90-23c	rs92.3	gsg92.9	C91-14	WSG93.1	C90-23c	rs92.3	gsg92.9	C91-14
SiO ₂	35.50	35.97	34.88	35.43	35.03	35.57	46.77	46.02	46.73	45.33
TiO ₂	1.98	1.97	2.97	18.40	2.75	5.14	0.88	1.10	1.42	0.85
Al ₂ O ₃	18.69	19.20	18.44	3.59	18.20	16.20	35.58	33.75	34.82	35.80
FeO	19.88	20.29	18.61	19.25	20.52	16.86	1.05	1.44	1.19	2.15
MnO	0.04	0.04	0.09	0.12	0.14	0.06	0.01	0.01	0.02	0.01
MgO	9.70	9.79	9.52	9.56	9.52	11.13	0.86	0.97	1.09	0.59
CaO	0.01	0.01	0.00	0.01	0.00	0.00	0.01	0.00	0.00	0.01
Na ₂ O	0.29	0.27	0.16	0.11	0.26	0.13	1.28	0.60	0.39	0.70
K ₂ O	8.35	8.39	9.93	10.13	9.77	10.10	9.34	11.03	11.87	10.84
Total	94.44	95.94	94.60	96.62	96.19	95.19	95.78	94.93	97.35	96.28
Formula proportions of cations based on 22 oxygen atoms										
Si	5.43	5.42	5.36	5.34	5.34	5.40	6.16	6.19	6.13	6.02
Ti	0.23	0.22	0.34	3.27	0.31	0.59	0.09	0.11	0.14	0.08
Al	3.37	3.41	3.34	2.66	3.27	2.90	5.52	5.35	5.39	5.61
Al(IV)	2.57	2.58	2.64	0.49	2.66	2.60	1.84	2.65	1.87	1.98
Al(VI)	0.80	0.83	0.70	0.54	0.61	0.30	3.68	2.70	3.52	3.63
Fe	2.54	2.56	2.39	2.43	2.62	2.60	0.12	0.16	0.13	0.24
Mn	0.00	0.01	0.01	0.02	0.02	0.30	0.00	0.00	0.00	0.00
Mg	2.21	2.20	2.18	2.15	2.16	2.14	0.17	0.19	0.21	0.12
Ca	0.00	0.00	0.00	0.00	0.00	0.00	0.00	0.00	0.00	0.00
Na	0.09	0.08	0.05	0.03	0.08	0.04	0.33	0.16	0.10	0.18
K	1.63	1.61	1.95	1.95	1.90	1.96	1.57	1.89	1.96	1.84
Fe/(Fe+Mg)	0.53	0.54	0.52	0.53	0.55	0.55	–	–	–	–

APPENDIX TABLE 2. Electron microprobe analyses

	Plagioclase				
	C90-23c core	C90-23c rim	gsg92.9 plag	C91-14 Kfs	
SiO ₂	64.57	62.87	63.36	63.82	62.29
Al ₂ O ₃	22.80	23.90	23.36	18.61	23.27
FeO	0.05	0.06	0.03	0.14	0.10
CaO	3.39	4.81	3.66	0.02	4.99
Na ₂ O	9.93	8.83	9.45	1.15	8.98
K ₂ O	0.09	0.04	0.09	15.16	0.16
Total	100.84	100.50	99.94	98.89	99.80
Formula proportioning of cations based on 8 oxygen atoms					
Si	2.83	2.77	2.80	2.97	2.77
Al	1.18	1.24	1.22	1.02	1.22
Fe	0.00	0.00	0.00	0.00	0.00
Ca	0.16	0.23	0.17	0.00	0.24
Na	0.84	0.75	0.81	0.10	0.77
Mole fraction of end-members					
K	0.01	0.00	0.01	0.90	0.01
Ab	0.18	0.24	0.79	0.10	0.77
An	0.82	0.76	0.20	0.00	0.22
Or	0.00	0.00	0.01	0.90	0.01

APPENDIX TABLE 3. Electron microprobe analyses

	C9023a core	C9023a rim	C9023c core	Garnet		gsg92.9 core	C91-14 rim	WSG93.1 core
				c9023c rim	rs92.3 rim			
SiO ₂	37.57	38.08	38.08	37.37	36.80	36.58	36.95	38.29
TiO ₂	0.02	0.04	0.03	0.02	0.02	0.01	0.02	0.00
Al ₂ O ₃	20.35	20.64	19.90	19.87	20.97	20.61	20.65	21.24
FeO	34.05	36.82	34.67	36.61	34.09	32.00	32.19	30.40
MnO	1.67	1.87	2.03	1.94	5.34	6.83	6.35	2.06
MgO	4.67	2.93	3.55	2.74	2.40	2.60	2.84	7.53
CaO	1.69	1.22	1.65	1.08	0.87	0.88	1.57	1.08
Total	100.00	101.60	99.92	99.62	100.51	99.52	100.60	100.60
Formula proportions of cations based on 12 oxygen atoms								
Si	3.01	3.03	3.06	3.04	2.97	2.99	2.98	2.99
Ti	0.00	0.00	0.00	0.00	0.00	0.00	0.00	0.00
Al	1.92	1.94	1.89	1.91	2.00	1.98	1.96	1.95
Fe	2.28	2.45	2.33	2.49	2.30	2.19	2.17	1.99
Mn	0.11	0.13	0.14	0.13	0.37	0.47	0.43	0.14
Mg	0.56	0.35	0.43	0.33	0.29	0.32	0.34	0.88
Ca	0.14	0.10	0.14	0.09	0.08	0.08	0.14	0.09
Mole fraction of end-members								
Gr	0.05	0.03	0.05	0.03	0.02	0.03	0.04	0.03
Py	0.18	0.12	0.14	0.11	0.10	0.10	0.11	0.28
Alm	0.74	0.81	0.77	0.82	0.76	0.72	0.70	0.64
Sp	0.04	0.04	0.05	0.04	0.12	0.15	0.14	0.04
Fe/(Fe+Mg)	0.80	0.88	0.85	0.88	0.89	0.87	0.86	0.44